Građevinski materijali i konstrukcije
Building Materials and Structures
journal homepage: www.buildingmaterialsstructures.com

https://doi.org/10.5937/GRMK2500010W UDK: 693.611

Original scientific paper

Improving the water permeability of mortar by using a hydrochar additive derived from coconut coir fiber

Eko Widodo[*1,2], Ariadne L. Juwono[1)], Ismail Budiman[2)], Subyakto[2)], Triastuti[2)], Utami D. Syafitri[3)]

[1)] Department of Physics, Faculty of Mathematics and Natural Science, University of Indonesia, Depok, Indonesia
[2)] Research Center for Biomass and Bioproducts, National Research and Innovation Agency, Indonesia
[3)] Department of Statistics and Data Science, Faculty of Mathematics and Science, IPB University, Bogor, Indonesia

Article history

Received: 30 July 2025
Received in revised form: 09 October 2025
Accepted: 14 October 2025
Available online: 10 November 2025

Keywords

additive,
hydrochar,
mortar,
water permeability,
mechanical properties

ABSTRACT

Mortar has been widely applied as a coating for various purposes on building infrastructures, including basements, water tanks, retaining walls, dams and building exteriors, where resistance to moisture and water is highly required. Various chemicals have been added to mortar to reduce its water permeability. However, they raise environmental problems, therefore, environmentally friendly additives are indispensable. The purpose of this study was to enhance the water resistance, compressive strength, and crack recovery ability of mortar with the addition of hydrochar from biomass. Hydrochar was prepared from the hydrothermal carbonization of coconut coir fiber at 150°C for 4 hours. The hydrochar was added to the mortar at different particle sizes and ratios to cement. Mortars were made by mixing cement, sand, water, superplasticizer, and hydrochar; and they were tested after 28 days. The results showed that the addition of 1 wt% hydrochar with a particle size of 150–250 μm reduced the water permeability of mortar, as evidenced by a 36.45% decrease in secondary water absorption and a 14.94% reduction in percentage of void. In addition, the compressive strength increased by 10.29% compared to the control mixture. Hydrochar can absorb water bubbles in the mortar mixture; however, excessive hydrochar causes the mortar to be more porous. The addition of hydrochar in mortar demonstrated superior crack recovery abilities because it functions as a connection medium to accelerate the recovery.

1 Introduction

Mortar, a widely used material in construction, consists of cement, aggregates, water, and optional additives or admixtures. A waterproof additive is added to the mortar immediately before or during mixing to modify the properties of mortar to make it more suitable for underwater conditions, thereby improving durability and construction efficiency. Water penetration in concrete reduces the material's strength and durability. Furthermore, it causes the corrosion of steel reinforcement in coastal locations. Mortar with low water permeability is the most effective variety for inhibiting water infiltration. Low water-permeability mortar is utilized in subterranean applications, such as basements, underground parking, high-rise buildings, water reservoirs, roof slabs, and flood-prone building areas.

In recent times, numerous researchers have studied water-permeability mortar. They used external membranes, surface coating, or integral waterproofing to make mortar with low water-permeability. The utilization of integral waterproofing admixtures aims to create a barrier; therefore, the water does not enter the concrete and mortar [1]. The use of hydrophobic agents created mortar impermeable to water [2]. The water absorption of concrete using Portland Cement Composite with a water-binder ratio of 0.40 and 1.5% admixture was measured 3% and 5% at 28 days. As a result, this concrete reduced the cost for the construction of water-resistance building [3]. Utilization of rice husk ash (RHA) and cementitious capillary crystalline waterproofing (CCCW) enhanced both the mechanical properties and impermeability of the mortar [4].

Several researchers investigated the utilization of biochar in mortar and concrete. For instance, substitution of 20% sand with biochar increased the flexural strength by 26% [5]. Furthermore, the addition of 1% biochar from peanut (PS) and hazelnut (HS) shells improved the flexural strength [6]. The application of biochar coating in fiber resulted in a reduction in the permeability of mortar [7]. Gupta et al. reported that the addition of biochar up to 2% reduced water absorption [8]. Furthermore, biochar-derived wood waste and food waste indicated greater efficacy in reducing the depth of water penetration [8].

* Corresponding author:
E-mail address: ekow004@brin.go.id

Coconut coir fiber (CCF) has generated interest as a potential reinforcement material because of its availability, cost-effectiveness, physical properties, reusability, and low density[9]. CCF, a widely commercialized product in tropical areas, offers a rich source of lignin, cellulose, and hemicellulose[10]. The potential of CCF in sustainable construction materials, especially regarding mortar composites, has been recognized as a significant area of focus. Adding CCF and other natural fibers to cementitious material reduced workability [11] and it became more porous [12]. It also decreased compression strength[13] and raised the tensile strength [14] and flexural strength [15]. It also made the material more resistant to impact [16] and accelerated the carbonation process [17]. Another study stated that the carbonization process transforms CCF into biochar, which enhanced the properties of mortar [18], [19], [20], [21], [22], [23], [24].

CCF, as a raw material for biochar, has 33.5% lignin[25]. The lignin content of CCF was similar to other materials commonly used as biochar raw materials, such as coconut shells with 27% lignin[26] and oil palm shells with 45.82% lignin [27]. Adding up to 2 wt% of biochar to cement has been shown in several studies to improve its mechanical properties, made it denser [28], more resistant to water[29], and enhanced crack recovery [30]. The factors, such as the percentage of biochar addition [3], raw material selection[8], carbonization methods [31],specific surface area, void volume, and particle size, significantly influenced research outcomes[32]. The researcher did not recommend adding biochar to more than 5% of the cement mass because it affected the strength[33].

Another material with similar properties to biochar is hydrochar, which is produced through hydrothermal carbonization (HTC). Both hydrochar and biochar share hygroscopic characteristics, making them both promising additives in mortar. Hydrochar, when compared to biochar, exhibits a lower carbon content, a lower ash content, a more uniform void size, a lower specific surface area, retains tensile strength, and is a more cost-effective manufacturing process [34]. Although significant research has been conducted on biochar in mortar, the application of hydrochar in this context is still largely unexamined. According to Hermawan et al. adding activated carbon from oil palm shells and hydrochar from empty palm fruit bunches to mortar made it stronger, better at absorbing pollutants, and better at healing micro-cracks [30].

The purpose of this study is to determine whether adding hydrochar from coconut coir fiber could increase the mortar's water permeability, compressive strength, and crack healing. This research evaluated 3 hydrochar particle sizes (75–150, 150–250, and 250–425 µm) and 3 hydrochar's content variation (1, 2, and 3wt%).

2 Materials and methods

2.1 Materials

This research used commercially available coconut coir fibers from West Java, Indonesia; Portland Cement Composites (PCC); fine aggregate from West Java, Indonesia; and Sikament®LN, as a superplasticizer.

2.2 Preparation of hydrochar

The hydrochars production included pretreatment of CCF and the hydrothermal carbonization process. First, CCF (Fig. 1a) was purified with water to eliminate contaminants. Then, it was placed into a 28-liter HTC rotary digester reactor (Fig.1b) at 150°C and maintained under autogenous pressure for 4 hours. After that, the hydrochars were collected from the reactor and they were dried in the oven at 60°C for 24. The dry hydrochar underwent grinding and sieving into different particle size ranges of 75–150, 150–250, and 250–425 µm (Fig. 1c).

2.3 Mix design of mortar

In this research, the mortar included cement, water, sand, super-plasticizer, and hydrochar. The ratio of cement to sand was 1:2.75 (by weight), water to cement was 1:2 (by weight), the percentage of super-plasticizer to cement was 1.5% (by weight), and the hydrochar content was 1, 2, and 3 % of the cement (by weight). Table 1 shows the mortar mix design.

Mixing was done in a digital mortar mixer with 5-liter capacity by Controls mixer (Fig.2). Water, cement, super-plasticizer, and hydrochar were mixed in the mixer at medium speed (140 rpm) for 30 seconds, then sand was added for 30 seconds at medium speed. The mixing was continued at high speed (285 rpm) for 1 minute. Then, the homogeneous mixture was put into cube molds (50 x 50 x 50 mm) and into cylindrical molds with a diameter of 100 mm and a height of 200 mm. After that, the mortar was removed from the mold after 24 hours and, it was immersed in water for 28 days to complete the curing process.

Figure 1. Preparation of hydrochar, a) coconut coir fiber (CCF), b) HTC rotary digester reactor, c) hydrochar

Table 1. Mix design of mortar

Code	Hydrochar			Cement, water, sand, superplsticizer (g)
	Ratio (wt%)	Weight (g)	Size (μm)	
C	-	-	-	
M11	1	5	250-425	
M12	2	10	250-425	
M13	3	15	250-425	Cement : 500
M21	1	5	150-250	Water : 250
M22	2	10	150-250	Sand : 1375
M23	3	15	150-250	Superplatisizer: 7,5
M31	1	5	75-150	
M32	2	10	75-150	
M33	3	15	75-150	

Figure 2. A digital mortar mixer

2.4 Mortar testing

Mortar testing in this study included density, compressive strength, water resistance, crack healing ability, and percentage of void area. Table 2 shows the details of the specimens for each test.

Table 2. Details of the specimens for each test

Test	Dimension	Remarks
Density	cube 50 x 50 x 50 mm	Specimens for compression tests
Compressive strength	cube 50 x 50 x 50 mm	After 28 days of water immersion.
Water penetration	cylinder D = 100 mm. t = 50 mm	After 28 days of water immersion.
	cylinder D = 100 mm. t = 25 mm	After 28 days of water immersion.
Void surface area	Square 15 x 15 mm	Cross-sectioned specimens
Crack healing ability	cube 50 x 50 x 50 mm	Specimens from compression tests

2.5 Density measurement

This study tested the density using a mortar cube of 50x50x50 mm in accordance with ASTM C642[35]. Five repetitions of each variation were tested. The density was calculated by dividing the mass by the volume of the specimen.

2.6 Compressive strength test

According to ASTM C109 [36] , this study conducted the compressive strength at 28 days using mortar cubes of 50 x 50 x 50 mm, 28 days. A universal testing machine, series 60 Static-Hydraulic Model 64.106, manufactured by MTS Criterion, was used (Fig. 3), with a speed of 0.002 mm/second. The tests used five repetitions of each variation.

2.7 Water permeability test

We conducted a water permeability test by measuring porosity, sorptivity, and percentage of surface voids. ASTM C 1585 [37] was used to assess sorptivity, and ASTM C642 [35] was used to measure porosity. This test used a digital microscope (KEYENCE VHX 6000)for microscopic analysis to identify the surface of the voids.

Figure 3. Compressive strength test

This study measured sorptivity using cylindrical test specimens, each measuring 100 mm in diameter and 50 mm in height. The specimens were dried in the oven at 50°C for three days to maintain a relative humidity of 80%. Next, the specimens were put in an isolated container for 15 days. During the preparation phase, the side surfaces of the test specimens were sealed with water-resistant materials such as electrical insulation or vinyl paint, and the top surface was covered with plastic. Then the specimens were positioned on supports with a water-filled container, ensuring a submersion depth of 1-3 mm from the bottom of the specimens. This study calculated the sorptivity value and collected data at interval of 1, 5, 10, 20,30, and 60 minutes; every hour up to 6 hours; and daily up to 9 days. The test scheme is shown in Fig 4.

This research used cylindrical specimens with a diameter of 100 mm and a height of 25 mm for the water penetration resistance test [35]. The specimen was heated at 110°C for 24 hours, weigh the specimen repeatedly until the difference between the last two results was less than 0.5%, then record the final result. Next, the specimens were immersed in water for a minimum of 48 hours and repeat the weight measurements from the initial heating phase. After this, they were boiled for 5 hours. Then they were put at room temperature for a minimum of 14 hours until they reached a temperature of 20 - 25°C, and then they were dried with a towel before weighing them. Lastly, they were submerged in water and weighed. This research used five repetitions for each variation of the water penetration resistance test.

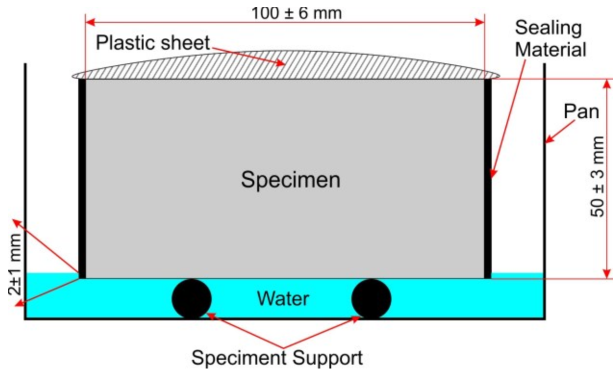

Figure 4. Sorptivity test scheme according to ASTM C1585

For the porosity test, the sample was cut into 15x15x5 mm,and a digital microscope was used to take pictures of each cross-section. This study used the ImageJ program to assess the percentage of void surface area.

2.8 Crack recovery ability

To evaluate the efficacy of crack healing in specimens, those exhibiting cracks with width between 10 and 200 µm were selected based on the outcome of a compressive strength test. The fracture width were first measured using a Dino-lite microscope AM2111. Then, the specimens underwent 14 cycles of wet-dry conditions, followed by extended monitoring for up to 60 days to further understand the crack healing process. The wet-dry cycles involved immersing the specimens in water for 12 hours, followed by exposure to ambient conditions for another 12 hours. This research assessed the crack widths (µm) throughout each cycle, allowing us to investigate on the progression of crack healing during the designated period.

3 Result and discussion

3.1 The chemical content of CCF

The chemical analysis of CCF revealed a significant lign in content of 36.13%. The chemical content obtained in this study is comparable with other results [32]. The high lignin content served as a suitable parameter for various applications, particularly as a raw material for hydrochar [38]. Table 3 presents a comparative examination of the chemical components of CCF in this study, considering previous research on CCF, coconut shell (CS), and oil palm shell (OPS).

Table 3. Comparison of chemical components of CCF with other raw materials

Chemical content	CCF (%)	CCF[25] (%)	CS[26] (%)	OPS[27] (%)
Holocellulose	60.86	53.4	55	43.77
Hemicelulose	27.24	37.9	34	23.96
Cellulose	33.62	15.5	21	19.81
Lignin	36.13	33.5	27	45.82

3.2 Properties of CCF and resulting hydrochar

The results of the yield and proximate analysis of hydrochar were presented in Table 4. Hydrochar produced through the HTC process exhibited a high yield of 77.66%, a low fixed carbon content of 16.69%, and a minimal ash content of 0.78%. The temperature and duration of the HTC process influenced these results [34]. Surface area testing using the BET method indicated a slight increase in the specific surface area of the hydrochar. The specific surface area of the hydrochar was measured at 5.529 m²/g, demonstrating a slight improvement compared to the specific surface area of coconut coir fibers at 2.700 m²/g. This value is lower than that of hydrochar derived from oil palm shell, which is 20.667 m²/g [27], and significantly lower than that of activated carbon, which is 1585.4 m²/g [39]. However, some studies suggest that higher temperature during hydrochar production can significantly enhance the material's porosity and surface area, leading to improved absorption capabilities. The result implies that while lower temperatures may preserve certain qualities, they might limit the overall potential of hydrochar for various applications. As suggested by Budiman et al. [27], higher temperature and longer HTC processes tend to decrease yield values, increase fixed carbon content, and enhance the specific surface area of hydrochar.

Table 4. Properties of raw CCF and resulting hydrochar

Properties	Unit	CCF	Hydrochar
Yield	%	-	77.66
Moisture content	%	-	5.50
Volatile matter content	%	-	82.53
Ash content	%	-	0.78
Fixed carbon content	%	-	16.69
Specific surface area	m²/g	2.70	5.53
Pore volume	cm^3/g	0.021	0.028
Tensile strength	MPa	86.08	28.72

Furthermore, tensile strength testing was conducted to measure the reduction in the tensile strength of hydrochar. The results indicated a tensile strength of 86.08 MPa for CCF, whereas hydrochar exhibited a reduced tensile strength of 28.72 MPa. The decrease in tensile strength of hydrochar is caused by the decomposition, degradation, transformation, and partial bonding of hemicellulose, cellulose, and lignin into other compounds during the HTC process [40].

3.3 Density and compressive strength of mortar

The addition of hydrochar only slightly impacted the density of the mortar (Fig. 5). The control mortar had a 1.97 g/cm^2 density, whereas the specimen densities varied from the lowest for M12 at 1.87 g/cm^2 to the highest for M22 at 2.06 g/cm^2. A reduction in void volume led to an increase in mortar density, while the porosity of hydrochar was responsible for the decrease. The variations in mortar density were insignificant [17], [45].

For every mortar variant, the compressive strength increased with the addition of hydrochar, as shown in Fig. 6. With a compressive strength rise to 33.39 MPa, the M22 specimen showed the most significant enhancement. The control mortar had a compressive strength of 23.39 MPa, and this value surpassed it by 42.79%. hydrochar's ability to absorb free water in the mortar mixture boosts its compressive strength. Absorption of free water in the mortar mixture can reduce air bubbles in the finished mortar [28].

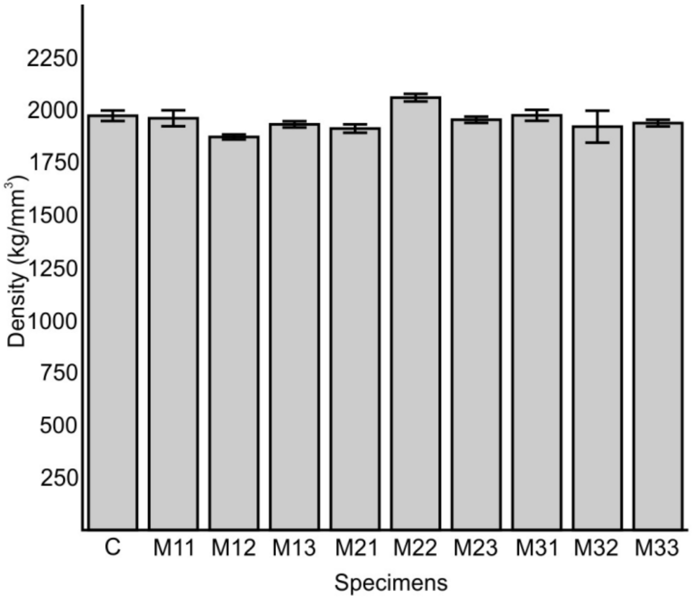

Figure 5. Density of mortar with variations in composition and particle size

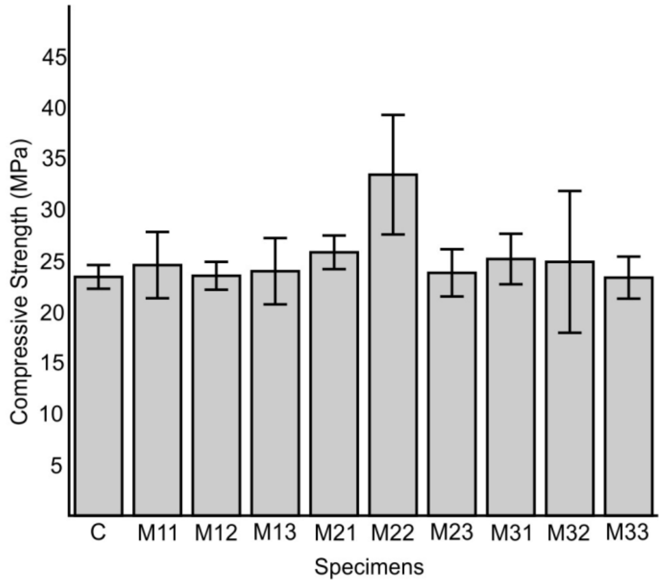

Figure 6. Compressive strength of mortar with variations in composition and particle size

3.4 Water permeability analysis

This research evaluated the water permeability to determine porosity (ASTM C 642) and to assess sorptivity (ASTM C 1585). The porosity or percentage of void, indicates the amount of water that can pass through the test specimen. The void percentage rose as the ratio of added hydrochar rose, as presented in Fig. 7. The void percentages for M21, M22, and M31 were 20.83%, 23.94%, and 24.25%, respectively. These results were lower than those of the control sample, which was a positive trend. Similar to biochar, hydrochar absorbed all free water present in the mortar paste [9]. This process has reduced the void content in the mortar [8]. However, excessive hydrochar addition can lead to an increased void percentage as the water-absorbing porosity of hydrochar raises the void percentage in the mortar. Fig. 8 displays the schematic model.

The addition of hydrochar impacted the sorptivity of mortars. Fig. 8 provides details about the sorptivity of mortar specimens, categorized into initial and secondary absorptions. Initial absorption is the specimen's ability to absorb water during the first 6 hours of the initial test, while secondary absorption is the specimen's ability to absorb water from 6 hours to 9 days of testing. M22 exhibited the smallest initial absorption value at 4.093×10^{-3} mm/√s.M22 had lower initial absorption values than the control specimen at 4.982×10^{-3} mm/√s. The high density and low porosity of M22 contributed to its ability to suppress initial absorption values. Regarding secondary absorption, M22 recorded a value of 2.658×10^{-3} mm/√s, higher than the control sample with a value of 1.841×10^{-3} mm/√s. The hydrochar content in mortar is starting to play a role in water absorption. On the other hand, M21 had a low secondary absorption value of 1.170×10^{-3} mm/√s because it had the fewest pores and only 1% hydrochar addition.

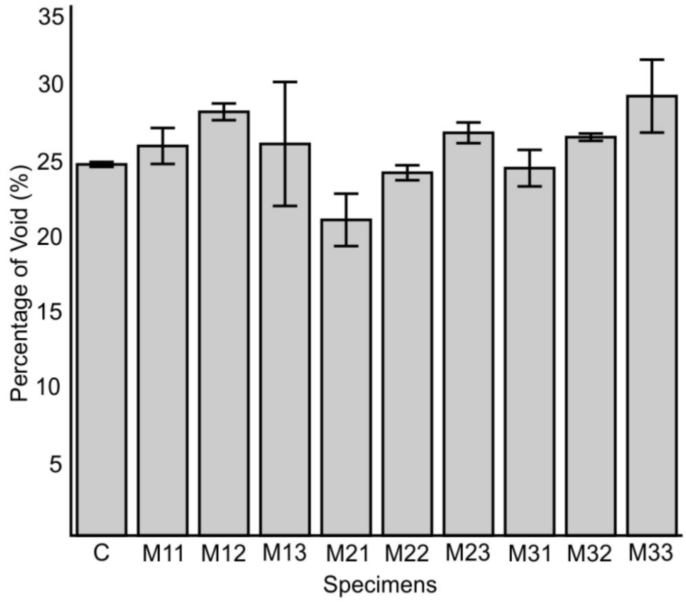

Figure 7. Percentage of mortar void with variations in composition and particle size

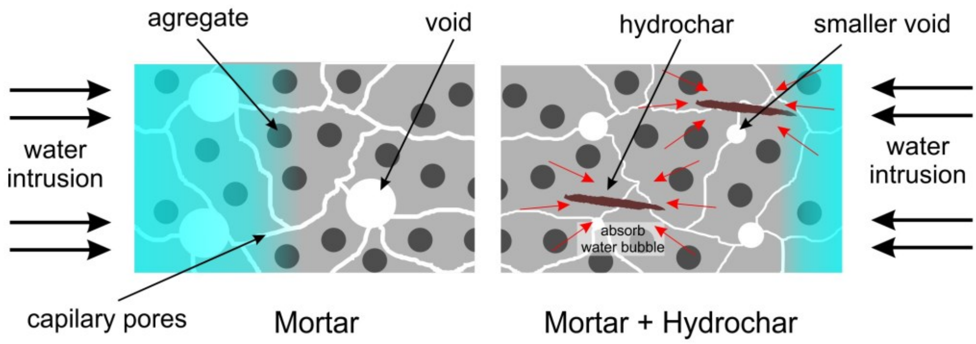

Figure 8. Schematic model of hydrochar absorbing free water in mortar mixture

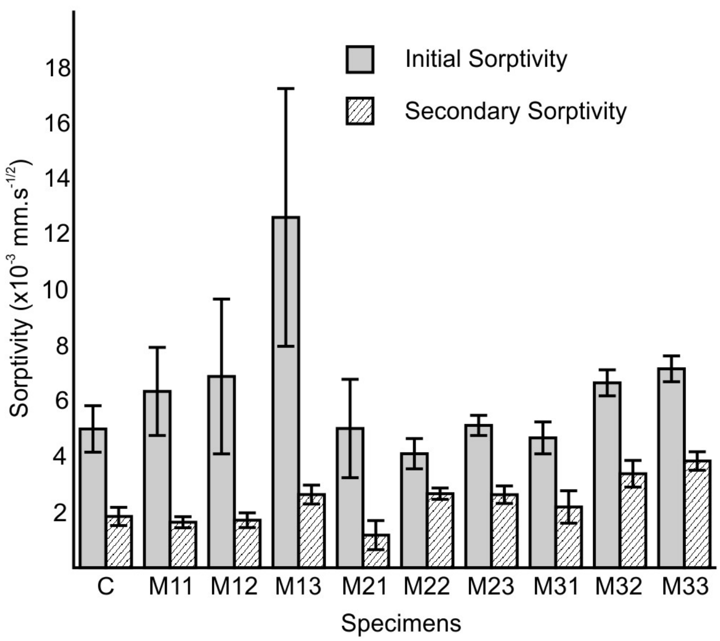

Figure 9. Sorptivity of mortar specimens

The results of microscopic analysis conducted on C, M21, M22, and M23 indicated that the percentage of void areas observed under the microscope did not correspond with the trend seen in porosity or sorptivity. The Fig. 9 and 10 showed that the addition of hydrochar correlated inversely with the percentage of void area observed.

According to ASTM C640, M23 had a small void area but, it had significant porosity. The elevated porosity of hydrochar resulted in a more significant increase in overall porosity upon 3% hydrochar rather than a decrease in void area.

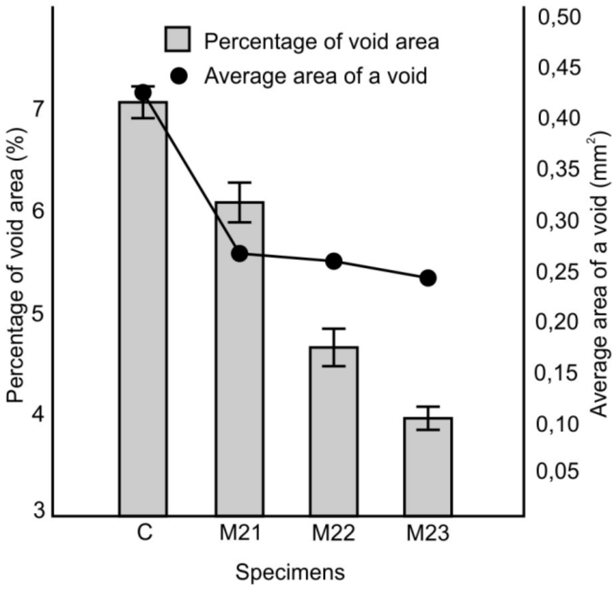

Figure 10. Percentage void area and average area of a void of mortars

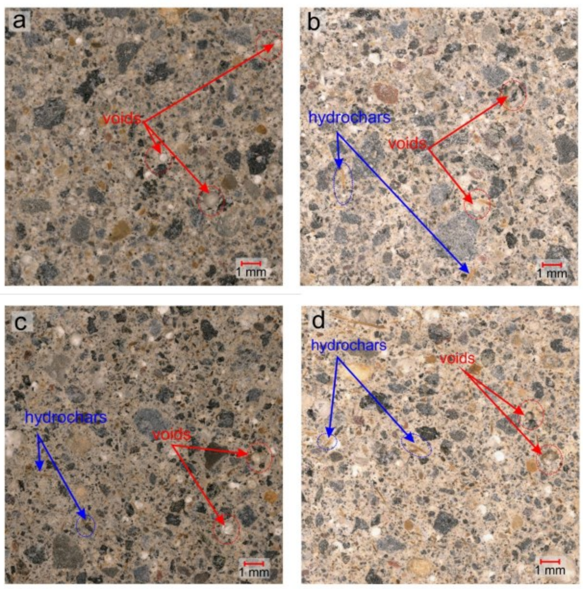

Figure 11. Cross-sections of mortar test specimens (a) control sample, (b) Mortar M21 with the addition of 1% hydrochar with size 150 - 250 µm, (c) Mortar M22 with the addition of 2% hydrochar with size 150 - 250 µm (d) Mortar M23 with the addition of 3% hydrochar size 150 - 250 µm

3.5 Crack recovery ability result

Table 5 presents crack recovery data after the wet-dry cycle, and Fig. 12 presents surface topography images illustrating crack recovery using the control and M22. According to Table 6, mortar with hydrochar demonstrated crack recovery abilities ranging from 5.65 to 31.4 µm within 14 days and 10.48 to 47.19 µm within 60 days. Hermawan et al.[30] obtained similar results using activated carbon from oil palm shells and hydrochar from empty palm fruit bunches. Calcium carbonate ($CaCO_3$) crystals and calcium silicate hydrate (CSH) are formed during advanced hydration processes that allow cracks to heal [46], [47]. The presence of crack-connecting media, such as fibers, accelerated crack recovery [48].

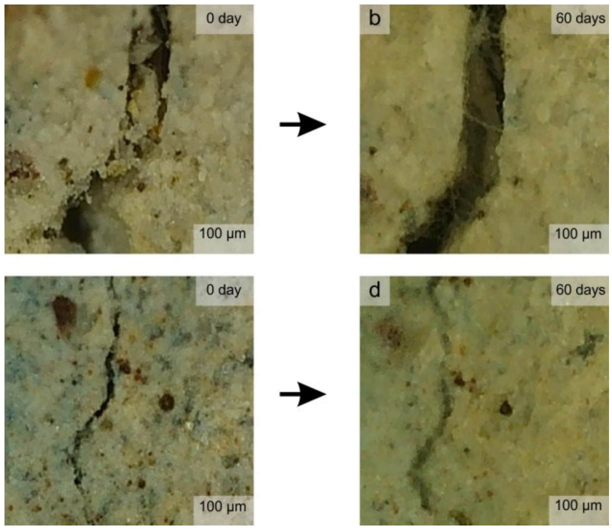

Figure 12. Microscopic photos of the recovery crack of mortar specimens after wet-dry cycle treatment: (a) initial condition, control specimen; (b) after 60 days; c) initial condition, M22 (d) after 60 days

Table 5. Crack recovery of mortars after wet-dry cycle treatment for 14 days and 60 days

Code	Crack recovery 14 days (µm)	Crack recovery 60 days (µm)
C	-1.13	-1.43
M11	18.98	28.29
M12	5.65	15.18
M13	8.97	10.48
M21	18.37	47.19
M22	13.76	17.58
M23	11.93	14.31
M31	18.34	20.32
M32	31.14	36.69
M33	13.30	15.63

During the initial hydration process, the hydrochar inhibited the formation of calcium carbonate and CSH. This let unreacted material help the crack recovery[49]. Gupta et al [48]. suggested that using additives like biochar accelerated the hydration process but also partially inhibited cement hydration, leaving unreacted materials functional for the crack recovery process. According to Tittelboom et al.[49], although crack recovery can effectively seal cracks, the formed calcium carbonate and CSH cannot fully restore the strength of the mortar.

4 Conclusion

- Hydrochar had a lower hemicellulose content than CCF.
- The addition hydrochar to mortar enhanced its characteristics.
- The optimum mortar performance was reached by adding 1% hydrochar with particle sizes ranging from 150 to 250 µm.
- The absorb of the mortar with 1% hydrochar was 4.998 x 10^{-3} mm/√s at first and 1.170 x 10^{-3} mm/√s at the second time.
- The void percentage of the mortar with 1% hydrochar was 20.83%.
- The compressive strength of the mortar with 1% hydrochar was 25.792 Mpa.
- The addition of hydrochar to mortar increased the crack recovery ability of mortar.
- Hydrochar became a crack-connecting media to accelerate crack recovery abilities.

The limitation of the study: This study investigated only the impact of coconut coir hydrochar on the water permeability and compressive strength of mortar under controlled laboratory conditions. The long-term performance under actual environmental conditions was not assessed. Only a single hydrochar type and preparation condition were evaluated, leaving the effects of other production parameters unexamined. Furthermore, micro-structural investigation was constrained, and additional durability factors, like carbonation were not examined. Future studies should focus on long-term durability and optimization of hydrochar characteristics.

Credit authorship contribution statement

EkoWidodo : conceptualization, methodology, investigation, data curation, data analysis, writing-original draft, review and editing.
Ariadne L. Juwono: supervision, conceptualization, investigation, review and editing
Ismail Budiman: supervision, conceptualization, investigation, review and editing
Subyakto; review and editing
Triastuti: review and editing
Utami D. Syafitri : data analysis

Conflict of interest

The author declare no conflict of interest.

Acknowledgements

The author (EW) would like to thank the SAINTEK scholarship program for support; the Integrated Laboratory of Bioproducts (ILAB) of Research Center for Biomass and Bioproducts - National Research and Innovation Agency of Indonesia (BRIN) and LPDP for support and facilities of this research.

References

[1] S. Jahandari, Z. Tao, M.A. Alim, W. Li, Integral waterproof concrete: A comprehensive review, Journal of Building Engineering 78 (2023) 107718. https://doi.org/10.1016/j.jobe.2023.107718.

[2] K. Ebrahimi, M.J. Daiezadeh, M. Zakertabrizi, F. Zahmatkesh, A.H. Korayem, A review of the impact of micro- and nanoparticles on freeze-thaw durability of hardened concrete: Mechanism perspective, Construction and Building Materials 186 (2018) 1105–1113. https://doi.org/10.1016/j.conbuildmat.2018.08.029.

[3] J. Li, S. Li, M. Aminul Haque, B. Chen, Water-resistance performance analysis of Portland composite concrete containing waterproofing liquid membrane, Journal of Building Engineering 76 (2023)106889. https://doi.org/10.1016/j.jobe.2023.106889.

[4] F. Ding, Y. Zhang, H. Wang, Z. Liu, W. Xu, Combined effect of rice husk ash and cementitious capillary crystalline waterproofing materials on the performance of mortar, Journal of Building Engineering 84 (2024) 108479. https://doi.org/10.1016/j.jobe.2024.108479.

[5] S. Praneeth, L. Saavedra, M. Zeng, B.K. Dubey, A.K. Sarmah, Biochar-admixtured lightweight, porous and tougher cement mortars: Mechanical, durability and micro-computed tomography analysis, Science of the Total Environment 750 (2021) 142327. https://doi.org/10.1016/j.scitotenv.2020.142327.

[6] R.A. Khushnood, S. Chaudhary, M. Ansari, A. Khan, M. Alnahhal, Carbonized nano/microparticles for enhanced mechanical properties and electromagnetic interference shielding of cementitious materials, Front. Struct. Civ. Eng. 10 (2016) 209–213. https://doi.org/10.1007/s11709-016-0330-5.

[7] H. W. Kua, S. Gupta, and C. Tan,Biochar as a Bond Enhancement in Fiber - Reinforced Mortar, Cem. Concr. Compos. 35 (2017) 589–594.

[8] S. Gupta, H. W. Kua, and H. J. Koh, Application of biochar from food and wood waste as green admixture for cement mortar, Science of the Total Environment, 619–620 (2018) 419–435. https://doi. org/10.1016/j.scitotenv.2017.11.044.

[9] F.R.C.R. Martinelli, F.C.G.F. Almeida, A.R.G. Andrade, M.T. Marvila, S.N. Monteiro, A review of the use of coconut fiber in cement composites, Polymers 15 (2023) 1309. https://doi.org/10.3390/polym15051309.

[10] R.M. Leão, S.M. Luz, J.A. Araujo, K. Novack, Surface treatment of coconut fiber and its application in composite materials for reinforcement of polypropylene, J. Nat. Fibers 12 (2015) 574–586. https://doi.org/10.1080/15440478.2014.984048.

[11] W. Ahmad, et al., Effect of coconut fiber length and content on properties of high strength concrete, Mater. 13 (2020) 1075. https://doi.org/10.3390/ma13051075.

[12] D. T. Tang, V. Lam; Vu, Kim Dien; Dang, Van Phi; Nguyen, Tai Nang Luong; Nguyen,Mechanical properties of building mortar containing pumice and coconut-fiber, in: Energy Management of Municipal Transportation Facilities and Transport, Springer International Publishing, Cham (2018) 648–659. https://doi.org/10.1007/978-3-030-19756-8_61.

[13] J. Ahmad, O. Zaid, M. S. Siddique, F. Aslam, H. Alabduljabbar, and K. M. Khedher,Mechanical and durability characteristics of sustainable coconut fibers reinforced concrete with incorporation of marble powder, Materials Research Express 8 (2021) 075505. https://doi.org/10.1088/2053-1591/ac10d3.

[14] M. Khan, A. Rehman, and M. Ali,Efficiency of silica-fume content in plain and natural fiber reinforced concrete for concrete road, Construction and Building Materials 244 (2020) 118382. https://doi.org/10.1016/j.conbuildmat.2020.118382.

[15] A. Yadav, S Kumar; Singh, An experimental study on coconut fiber reinforced concrete Sanjay, Trends in

Civil Engineering and Its Architecture 2 (2018) 2250–2254. https://doi.org/10.32474/tceia.2018.02.000126.
[16] C. L. Hwang, V. A. Tran, J. W. Hong, and Y. C. Hsieh,Effects of short coconut fiber on the mechanical properties, plastic cracking behavior, and impact resistance of cementitious composites, Construction and Building Materials 127 (2016) 984–992. https://doi.org/10.1016/j.conbuildmat.2016.09.118.
[17] M. Ramli, W. H. Kwan, and N. F. Abas,Strength and durability of coconut-fiber-reinforced concrete in aggressive environments, Construction and Building Materials 38 (2013) 554–566. https://doi.org/10.1016/j.conbuildmat.2012.09.002.
[18] J. Waluyo *et al.*,Characterization of biochar briquettes from coconut shell with the effect of binder: Molasses, cow manure and horse manure, Evergreen 10 (2023) 539–545. https://doi.org/10.5109/6782158.
[19] M. Siregar, S, Pemanfaatan kulit kerang dan resin epoksi terhadap karakteristik beton polimer." Medan: Thesis Universitas Sumatera Utara (2009).
[20] N. B. Prihantini, N. Rakhmayanti, S. Handayani, W. Sjamsuridzal, W. Wardhana, and Nasruddin,Biomass production of Indonesian indigenous Leptolyngbya strain on NPK fertilizer medium and its potential as a source of biofuel, Evergreen 7 (2020) 593–601. https://doi.org/10.5109/4150512.
[21] A. F. Ridassepri, F. Rahmawati, K. R. Heliani, Chairunnisa, J. Miyawaki, and A. T. Wijayanta, Activated carbon from bagasse and its application for water vapor adsorption, Evergreen 7 (2020) 409–416. https://doi.org/10.5109/4068621.
[22] M. Sultan, I. I. El-Sharkawl, T. Miyazaki, B. B. Saha, and S. Koyama,Experimental study on carbon-based adsorbents for greenhouse dehumidification, Evergreen 1 (2014) 5–11. https://doi.org/10.5109/1495157.
[23] F. Jerai, T. Miyazaki, B. B. Saha, and S. Koyama,Overview of adsorption cooling system based on activated carbon–alcohol pair, Evergreen 2 (2015) 30–40. https://doi.org/10.5109/1500425.
[24] S. Gupta, P. Krishnan, A. Kashani, and H. W. Kua, Application of biochar from coconut and wood waste to reduce shrinkage and improve physical properties of silica fume-cement mortar, Construction and Building Materials 262 (2020) 120688. https://doi.org/10.1016/j.conbuildmat.2020.120688.
[25] Y. Kondo and M. Arsyad,Analisis kandungan lignin, sellulosa, dan hemiselulosa serat sabut kelapa akibat perlakuan alkali, INTEK: Jurnal Penelitian 5 (2018) 94–97. https://doi.org/10.31963/intek.v5i2.578.
[26] D. Tamado *et al.*,Sifat termal karbon aktif berbahan arang tempurung kelapa, in: Seminar Nasional Fisika Universitas Negeri Jakarta (2013) 73–81.
[27] I. Budiman, D. Hermawan, F. Febrianto, G. Pari, and Subyakto, Char properties and pollutant adsorption capability of oil palm shell using hydrothermal process, Biomass Conversion and Biorefinery 9 (2019) 681–688. https://doi.org/10.1007/s13399-019-00394-5.
[28] T. Han, Application of peanut biochar as admixture in cement mortar, IOP Conf Ser Earth Environ Sci531 (2020) 1. doi: 10.1088/1755-1315/531/1/012061.
[29] S. Gupta, H. W. Kua, and S. D. Pang, Effect of biochar on mechanical and permeability properties of concrete exposed to elevated temperature, Construction and Building Materials 234 (2020) 117338. https://doi.org/10.1016/j.conbuildmat.2019.117338.
[30] D. Hermawan *et al.*, Enhancement of the mechanical, self-healing and pollutant adsorption properties of mortar reinforced with empty fruit bunches and shell chars of oil palm, Polymers 14 (2022) 14030410. https://doi.org/10.3390/polym14030410.
[31] K. Tan, X. Pang, Y. Qin, and J. Wang,Properties of cement mortar containing pulverized biochar pyrolyzed at different temperatures, Construction and Building Materials 263 (2020) 120616. https://doi.org/10.1016/j.conbuildmat.2020.120616.
[32] S. Gupta and H. W. Kua,Carbonaceous micro-filler for cement: Effect of particle size and dosage of biochar on fresh and hardened properties of cement mortar, Science of the Total Environment 662 (2019) 952–962. https://doi.org/10.1016/j.scitotenv.2019.01.269.
[33] S. S. Senadheera *et al.*,Application of biochar in concrete – a review, Cement and Concrete Composites 143 (2023) 105204. https://doi.org/10.1016/j.cemconcomp.2023.105204.
[34] H. S. Kambo and A. Dutta, A comparative review of biochar and hydrochar in terms of production, physico-chemical properties and applications, Renewable and Sustainable Energy Reviews 45 (2015) 359–378. https://doi.org/10.1016/j.rser.2015.01.050.
[35] ASTM, Standard Test Method for Density, Absorption, and Voids in Hardened Concrete, ASTM C642-13, ASTM International, West Conshohocken, PA (2013).
[36] ASTM, Standard Test Method for Compressive Strength of Hydraulic Cement Mortars (Using 2-in. or [50 mm] Cube Specimens), ASTM C109/C109M-02, ASTM International, West Conshohocken, PA (2002).
[37] ASTM, Standard Test Method for Measurement of Rate of Absorption of Water by Hydraulic-Cement Concretes, ASTM C1585-13, ASTM International, West Conshohocken, PA (2013).
[38] C. Senthil and C. W. Lee, “Biomass-derived biochar materials as sustainable energy sources for electrochemical energy storage devices,” *Renewable and Sustainable Energy Reviews*, vol. 137, no. December 2019, p. 110464, 2021, doi: 10.1016/j.rser.2020.110464.
[39] J. Miyawaki *et al.*, “Influence of pore size and surface functionality of activated carbons on adsorption behaviors of indole and amylase,” *Evergreen*, vol. 3, no. 2, pp. 17–24, 2016, doi: 10.5109/1800868.
[40] G. Garrote, H. Domínguez, and J. C. Parajó, “Hydrothermal processing of lignocellulosic materials,” *Holz als Roh - und Werkstoff*, vol. 57, no. 3, pp. 191–202, 1999, doi: 10.1007/s001070050039.
[41] Sudarmanto *et al.*, “Effect of cold-water treatment and hydrothermal carbonization of oil-palm-trunk fibers on compatibility with cement for the preparation of cement-bonded particleboard,” *Wood Mater Sci Eng*, vol. 17, no. 6, pp. 979–988, 2022, doi: 10.1080/17480272.2021.1983871.
[42] S. Masoumi, V. B. Borugadda, S. Nanda, and A. K. Dalai, “2021-Hydrochar A Review on Its Production Technologies.pdf,” *Catalysts*, vol. 11, no. Figure 1, p. 939, 2021.
[43] E. Hermiati, L. Risanto, M. Lubis, R.P.B. Laksana, A.R. Dewi, Chemical characterization of lignin from kraft pulping black liquor of Acacia mangium, AIP Conference Proceedings 1803 (2017) 020003. https://doi.org/10.1063/1.4973132.
[44] J. Lamaming, R. Hashim, O. Sulaiman, C. P. Leh, T. Sugimoto, and N. A. Nordin, “Cellulose nanocrystals isolated from oil palm trunk,” *Carbohydr Polym*, vol.

127, pp. 202–208, 2015, doi: 10.1016/j.carbpol.2015.03.043.

[45] H. W. Kua and S. M. H. Tan, "Novel typology of accelerated carbonation curing: using dry and pre-soaked biochar to tune carbon capture and mechanical properties of cementitious mortar," *Biochar*, vol. 5, no. 1, Dec. 2023, doi: 10.1007/s42773-023-00234-w.

[46] T. Qureshi and A. Al-Tabbaa, "Self-Healing Concrete and Cementitious Materials," in *Advanced Functional Materials*, IntechOpen, 2020. doi: 10.5772/intechopen.92349.

[47] E. T. Rodriguez, I. G. Richardson, L. Black, E. Boehm-Courjault, A. Nonat, and J. Skibsted, "Composition, silicate anion structure and morphology of calcium silicate hydrates (C-S-H) synthesised by silica-lime reaction and by controlled hydration of tricalcium silicate (C3S)," in *Advances in Applied Ceramics*, Maney Publishing, Oct. 2015, pp. 362–371. doi: 10.1179/1743676115Y.0000000038.

[48] S. Gupta, H. W. Kua, and S. D. Pang, "Healing cement mortar by immobilization of bacteria in biochar: An integrated approach of self-healing and carbon sequestration," *Cem Concr Compos*, vol. 86, pp. 238–254, Feb. 2018, doi: 10.1016/j.cemconcomp.2017.11.015.

[49] K. Van Tittelboom, E. Gruyaert, H. Rahier, and N. De Belie, "Influence of mix composition on the extent of autogenous crack healing by continued hydration or calcium carbonate formation," *Constr Build Mater*, vol. 37, pp. 349–359, 2012, doi: 10.1016/j.conbuildmat.2012.07.026.